Modular Design, Communication and Control Systems of a 3D-printed Humanoid Robotic Hand

Ivan Chavdarov, Bozhidar Naydenov, Valentin Nikolov, Ivaylo Georgiev

***Abstract*—This article presents an innovative approach for developing the mechanical and control systems of humanoid 3D-printed hand with fingers, based on a modular principle. The novelty is in creating the 3D printed fingers as a single assembled component and embedding the actuators and control elements, thus making it a complete independent module. The new approach allows the implementation of the same software and actuating components to be used in finger modules with different individual sizes and joint constraints. The mechanical and control system of the hand is developed and a working prototype is created. It is described how to adjust and control the position of fingers with different sizes and joint constraints. The communication of the modules with the developed software is described. The repeatability of finger movement is studied and the force that each finger is capable of exerting during folding is measured. Functional experiments are performed and discussed.**

***Index terms*—Humanoid hand, control system, communication, 3D printing, modular design.**

I. Introduction

This work presents the development of an innovative humanoid 3D printed hand focusing on the software and communication systems of the created prototype.

The development of 3D printing technologies has led to the emergence of new constructive solutions for creating objects with a complex shape at a low cost. This approach allows the creation of humanoid robotic hands with personalized shape and dimensions [1, 2, 3]. An important advantage of additive manufacturing is that it quickly creates functional models that, after conducting experiments, can be modified and produced again. This quality is often used to verify results when solving optimization problems [4].

Manuscript received November 2, 2023; revised December 18. Date of publication March 18, 2024. Date of current version March 18, 2024.

I. Chavdarov is with the Faculty of Mathematics and Informatics, Sofia University, “St. Kliment Ohridski” and Institute of Robotics, Bulgarian Academy of Sciences, Sofia, Bulgaria (e-mail: ivannc@uni-sofia.bg).

B. Naydenov is with the Institute of Robotics, Bulgarian Academy of Sciences, Dassault Systemes, Sofia, Bulgaria (e-mail: Bozhidar.naydenov@3ds.com).

V. Nikolov is with the Institute of Robotics, Bulgarian Academy of Sciences and Sensata Technologies, Sofia, Bulgaria (e-mail: vnn@sensata.com).

I. Georgiev is with the Institute of Robotics, Bulgarian Academy of Sciences, Sofia, Bulgaria (e-mail: rainship@gmail.com).

The paper was presented in part at the International Conference on Software, Telecommunications and Computer Networks (*SoftCOM*) 2023.

Digital Object Identifier (DOI): 10.24138/jcomss-2023-0168

Finger actuators are important for the design, control and operation of the hand. Motors with small dimensions and less mass are preferred. In the literature are described prostheses with different types of actuators: linear motors [6, 10]; servo motors [11]; DC motors [5, 9]; and pneumatic cylinders [12, 13]. Important parameters of actuators that are investigated are: minimum and maximum speed, accuracy, repeatability, dimensions, weight and cost [3].

The human hand is capable of complex movements, and for this reason it is necessary for humanoid robotic hands to possess a large number of degrees of freedom (DOF). In [12] and [13] a hand with 20 DOF is presented, and in [14] with 16 DOF. These hands can realize complex movements, but the pneumatic actuation of [12, 13] requires devices located outside the palm of the hand, which does not allow it to be used as a prosthesis. In addition, the large number of DOF complicates mechanical design and control. Due to these facts, many researchers are looking for design solutions with a small number of degrees of freedom [1, 3, 15, 16] which can realize sufficiently reliable and adaptive grasping of objects. The design of a finger with one motor and a lever system that realizes dependent movement of the phalanges is presented in [15], where is shown that dependent movements of the phalanges can be used to reliably grasp cylindrical objects. In [16], a 3D-printed hand is described whose fingers are actuated by threads and elastic elements. The movements of the phalanges of each finger are again dependent.

Other important aspects in creating humanoid robotic hands are their sensory and control systems. According to [17], the skin of the human hand is saturated with tactile sensors, with the largest number per unit area in the fingertips. Such sensitivity is still technologically difficult to implement. The robotic arm presented in [9] uses three types of sensors: a force sensor; Hall effect sensor; and strain sensors in the tendons. Some prostheses are controlled by electromyography (EMG) sensors [18], and humanoid robot hands are often controlled using sensory gloves [19]. A disadvantage of EMG sensors is that it is necessary to calibrate and adjust the sensor for each person in order to use it correctly. In [19], a 3D-printed sensor glove with 10 degrees of freedom is considered, which is used to control a humanoid robotic hand. It has advantages related to low cost and low energy consumption. In [20], a control strategy is presented that uses a Leap Motion Controller that captures the joint angles of the human hand in real time. Other sensors that are often used in humanoid hands are: cameras [5], tactile arrays [21], potentiometers [22], accelerometers and distance and pressure sensors [23].

A major problem in the development of humanoid hands is the limited volume in which the mechanical components, sensors and controllers must be located. For this reason, solutions are sought in which fewer and smaller hardware components are used [24]. Hand control is implemented with different types of hardware depending on their purpose. Microcontrollers connected to a wireless (Bluetooth) connection are used in [10]. Some of the anthropomorphic hands are controlled with the Robot Operating System (ROS), which contains a set of software libraries for building applications [25]. Control software includes PC-based control systems [26] and advanced techniques such as deep learning and neural networks [27].

Industrial production has proven the benefits of implementing a modular design. In recent years, developments have appeared that apply the modular principle to the design of humanoid robotic hands. In [28], a 3D-printed humanoid hand based on a modular design that uses flexible material for the fingers and the palm is presented. It is actuated by threads and the motors are outside the palm. The HERI II hand [29] consists of modular fingers, with a single drive via transmission, and is equipped with a precision grip sensory system that includes absolute position measurements, a contact pressure sensor on the finger phalanges, and motor current sensing. The drive modules of this hand are too big, and the HERI II arm has a mass of 1603g, making it unsuitable for prosthetic use. In [30] a modular design for a prosthetic hand with finger- and wrist-level modularity is proposed, which allows for the removal and attachment of thread-driven fingers without the need for tools, reconnection of threads, and rewiring. The design allows the motors to be placed outside the hand to remotely actuate the threads that drive the fingers.

The following conclusions can be drawn from the literature review:

- 3D printing technology has many advantages for developing prototypes such as: creation of complex shapes; personalized design; and low cost and mass, which makes it attractive for creating robotic humanoid hands.
- There are two trends in the development of humanoid hands in terms of degrees of freedom. One seeks to develop complex models with a large number of DOF, and the other tries to achieve sufficient functionality with a small number of DOF. The authors believe that a reasonable compromise should be found, with each finger driven by at least one motor.
- Control and drive systems are implemented with different approaches depending on the specific application and design.
- The software and communication systems used in the humanoid robotic hands play key role in their development and applications.
- The application of modular design in humanoid hands will lead to better maintainability and servicing, improved reliability, and other advantages.

The conclusions drawn motivate the authors to create a prototype and explore a new design of a 3D-printed hand based on fingers built on a modular principle. The work presents a novel approach to the design of humanoid robotic hands, involving directly assembled fingers, modular hardware and software that allow the control of fingers of different sizes and joint constraints. According to the reviewed literature, there are no humanoid hands with fully autonomous finger modules.

It is created a finger design with assembled joints, which is only possible with 3D printing technology, using specially designed contact surfaces between the elements. The novelty of this methodology is confirmed by a published patent [31] from one of the authors. Another important advantage of 3D printing technology is that it allows the creation of fingers with individual shapes, sizes and joint constraints, at a very low cost. This expands the application possibilities of the hand in both robotics and prosthetics.

From the literature, it can be seen that existing servo motors that can realize sufficient torque are too large for the limited space of the palm. This necessitates the development of a new hardware, described in the article, and the usege of small DC gearmotors with high torque. The modular design also facilitates the development of the software and communication systems of the hand, because they can be replicated for hands or grippers with different number and size of fingers. The novelty of the software is related to its design, which allows easy readjustment when the sizes and joint constraints of the fingers change.

This work is a continuation and expansion of the scope of the article "Design of a 3D-printed Humanoid Robotic Hand" [3], where are given functional experiments and comparison of the design of the developed hand with other similar 3D-printed hands, in terms of DOF and mass.

The structure of the article is as follows: In I is presented the development, advantages and problems in 3D printed humanoid hands according to refereed literature sources from the last 10 years. Section II introduces the idea of the mechanical design of modular fingers and the means of producing them with a 3D printer as assembled components. The development of new hardware for individual finger control, which is built into the 3D printed module itself is presented in section III. The elements for communication between the modules and the control computer are given: In section IV is presented finger control software that allows for individual parameters to be set and section V describes and conducts an experiment on the repeatability of the movements of a finger in a predetermined sequence for folding of its phalanges. The forces realized by the tips of the fingers are measured. Section VI presents conclusions from the conducted experiments, guidelines for improving the design, advantages and disadvantages of the proposed approach.

II. Modular Design of the Humanoid Robotic Hand

The fingers of the humanoid hand are built on a modular principle, which covers its mechanical, sensory, and control systems (Fig. 1). The finger is composed of six 3D-printed elements: body with phalanges - 1; lid - 2; driving drum - 3; tension roller - 4; pressing cap - 5; and moving cap - 6. These parts are manufactured using FDM 3D-printing technology. The manufacturing process can be seen in video 1: https://www.youtube.com/watch?v=6XNhMk1xJKU. The body has a specific shape, which includes the phalanges and joints of the finger, and it is produced already assembled, see Fig. 2 b) and video 2: https://www.youtube.com/watch?v=SOvD6ft-eT8. The method of its creation is described in [3].

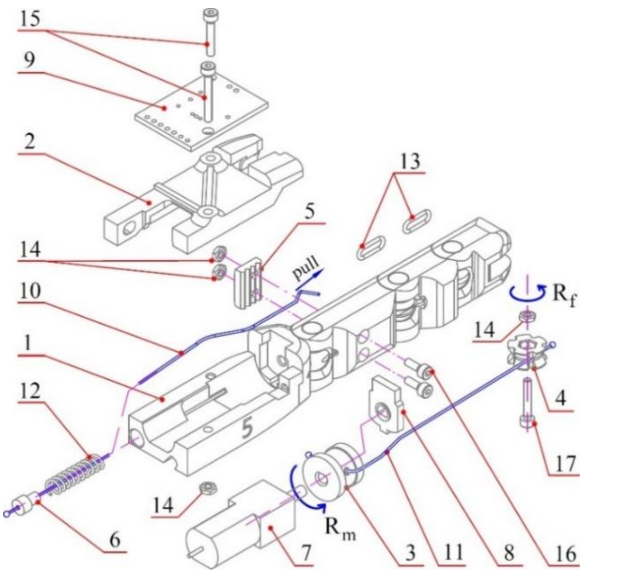

Fig. 1. Main components of a finger 1- finger body; 2 – lid; 3- driving drum; 4 - tension roller; 5 - pressing cap; 6 - moving spring cap; 7 – gear motor; 8 – resistive potentiometer; 9 - printed circuit board (PCB); 10 and 11 – threads; 12 – spring; 13 – rubber bands; 14 to 17 – fasteners. (from [3]).

The output shaft of the gearmotor 7 rotates the drum 3 (rotation R_m Fig. 1). One end of drive thread 11 is firmly attached to the drum, and passes through the holes of the individual phalanges of finger 1. The second end of thread 11 is connected to tension roller 4 (see Fig. 1 and 2). The thread 10 is intended for the unfolding of the finger, which is carried out by means of spring 12. In addition to spring 12, elastic elements 13 are used for the unfolding of the remaining two phalanges.

The initial length of spring 12 can be smoothly adjusted by pulling it with thread 10 which is then fixed with the pressing of cap 5. The initial length of the elastic elements 13 is obtained from the distance between the teeth located in adjacent phalanges (Fig. 3).

This distance is selected experimentally for each finger. Considerations for this choice are given in section V "Experiments and results".

Table I shows basic parameters of humanoid hands, known from the literature, based on the systematization criteria proposed in [32] for evaluating the qualities of robotic hands. Important criteria are the number of used motors, the mass of the hand, the possibility of realizing a power grip, and others.

According to [32] commercial hands used for prostheses have a small number of motors, which cannot always satisfy the requirements for achieving movements close to those of the human hand. Where as, other hands from the literature have a

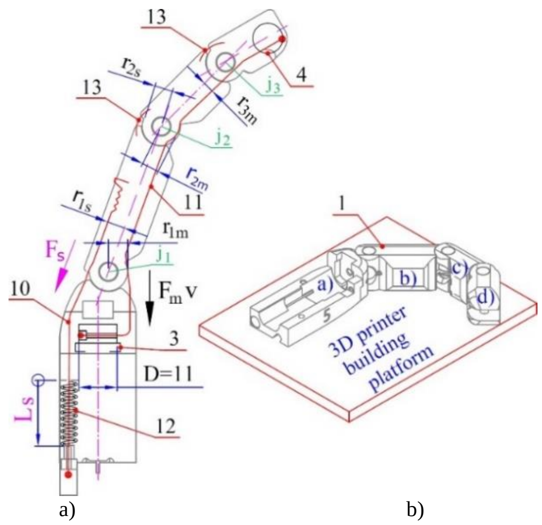

Fig. 2. a) Trajectories of the threads in the finger and placement of elastic elements, 1- finger body; 3- driving drum; 4 - tension roller; 10 and 11 – threads; 12 – spring; 13 – rubber bands; b) finger placement on the 3d printer building platform; (from [3])

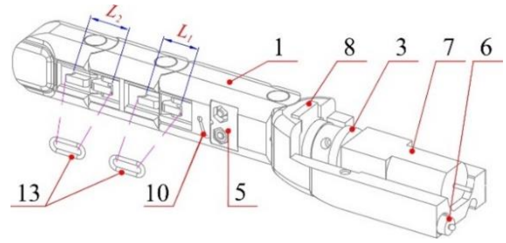

Fig. 3. Distances L_1 and L_2 which set the initial tension of elastic elements 13; 1 - finger body; 3- driving drum; 5 - pressing cap; 6 - moving spring cap; 7 – gear motor; 8 – resistive potentiometer; 10 – thread; 13 – rubber bands.

TABLE I
COMPARISON OF SIMILAR HUMANOID ROBOTIC HANDS

Name of the hand	DOF	Weight [kg]	Fingers	Modularity	Location of the motors in the palm
KIT Hand [5]	2	0.377	5	No	Yes
SARAH Hand [33]	10	4.9	3	Yes	no palm
Shadow Hand [33]	20	4.3	5	No	No
DLR Hand I [33]	16	1.8	4	Yes	3 motors in the palm
Gifu Hand III [34]	16	1.7	5	Yes	In the palm and in the fingers
Low-cost hand [12]	20	0.66	5	Yes	No
Cable Driven Humanoid Hand [35]	5	0.430	5	No	Yes
Hand presented in current work	*5*	*0.324*	*5*	*Yes*	*Yes, all 5 motors in the palm*

According to [32] commercial hands used for prostheses have a small number of motors, which cannot always satisfy the requirements for achieving movements close to those of the human hand. Where as, other hands from the literature have a

III. Control and Communication System

Every finger has its own control module, which is mounted in its base (Fig. 1). The modules of all the fingers are identical, which is an essential aspect of the modular concept of the design and allows every finger to be controlled independently. The main components of every control board are: 8-bit PIC12F1822 controller, H-bridge driver integrated in a single chip Sip2100, Pololu Micro Metal Gearmotor, Panasonic's resistive encoder EVW-AE4001B14 and communication protocol. Every finger is connected to a common multifunctional I2C USB-ISS communication device and a personal computer. The brushed DC motor has the following characteristics: 32 RPM; 120 mA with no load and 125 oz-in (9 kg-cm) and 1.6A at stall; intended for use at 6V; and it has a 1000:1 metal gearbox. The block and schematic diagram are given in Fig. 4 and Fig. 5.

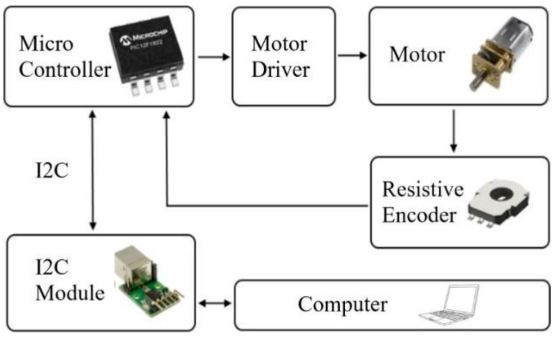

Fig. 4. Electronic components of the finger and the connection between them.

An 8-bit PIC12F1822 controller has only 6 I/O ports, but it provides all necessary peripherals for the testing and validation of the functionality of the fingers and the entire hand. Two of the outputs are used to control the speed and direction of the DC motor by means of the full H-bridge driver. The speed of the motor is controlled with PWM and its motion depends on the logical levels of the two outputs. If they are similar the motor remains stationary and if they are different it rotates in the corresponding direction. The finger position is determined from the feedback of the resistive encoder EVW-AE4001B14, which is coupled to the drive-shaft of the motor. The resistance is in the range 0-10[kΩ] when turning from 0 to 343°. The control is fit on a 30x22[mm] board, position 9 in Fig. 1, and is mounted on the finger with bolts. It is powered with 5[V] from a common external power supply. The value of the resistive encoder is read by a 10 bit analogue to digital converter (ADC) and is converted to least significant bit numbers (LSB). This determines the resolution of the system with the used voltage and resitance of the encoder.

The gearmotor used can be coupled with a magnetic encoder for the control feedback. Preliminary experiments show that if several motors with magnetic encoders are used in close proximity to each other, signal cross-talk occurs. For this reason, a resistive feedback encoder was chosen, where interference is not observed. The selected resistive encoder also has very good operating life of minimum 1000 000 cycles.

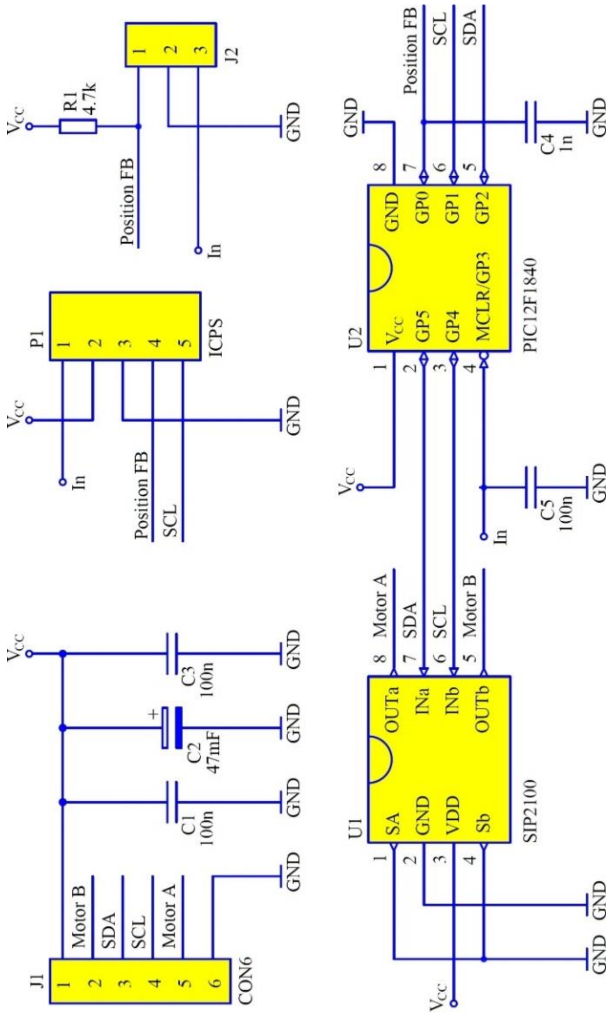

Fig. 5. Electronic diagram of the finger module.

The communication between the individual fingers and a USB-ISS master module is based on the I2C protocol with each finger being an I2C slave module with its unique identification number (slave address). In order to have full control of all fingers, it is necessary to use a separate module that can form different finger configurations, control the speed of the movements, and monitor for collisions and configurations where movements are limited.

Depending on the requirements there can be different approaches for developing such a platform. For the purposes and current development stage of the hand, a USB-ISS master interface module is connected to a computer running LabVIEW, and I2C commands are transmitted in order to conduct experiments with the hand. This module is a multifunctional USB device; once connected, it is recognized as a virtual serial port in Windows. Specific commands can be used to configure USB-ISS for one of the supported modes/interfaces. A block diagram of the communication between the fingers and the control platform (computer) is presented in Fig. 6.

This approach has advantages especially in the initial stages of the development process, since any programming language can be used and the use of an additional embedded hardware platform is not required.

Desktop programming also provides benefits in terms of the visualization and presentation of results. When the development process is finished, the acquired control data can be integrated into a specific embedded hardware platform situated on the hand itself. In this way, the external control of the hand could be reduced to simple commands like "move the fingers to the desired configuration", and the whole process of individual finger control, speed control, etc. can be compiled into the integrated hardware module.

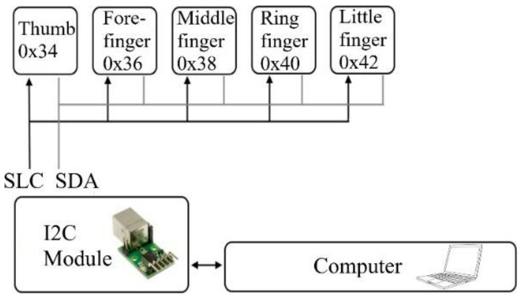

Fig. 6. Communication block diagram.

The USB-ISS I2C interface is based on exchanging hexadecimal single-byte codes. Read and write commands can be sent to the fingers. The identifiers for each finger are as follows: thumb 0x34; index 0x36; middle 0x38; ring 0x40; little finger 0x42. The following package is as an example of how a read command can be sent to a particular finger via USB-ISS:

0x55 0x32 0x01 0x01 0x02

The description of the bytes is as follows: 0x55 – the specific code of USB-ISS to set read/write mode on the I2C bus; 0x32 – the slave address of the device for which the command is intended; 0x01 – the specific register/function to be executed by the device (finger); 0x01 – the number of data bytes to be transmitted, in this case one byte; followed by a series of data bytes that are sent to the finger, in the example only one byte with the value 0x02.

Reading from a specific register is done in a similar way. An example of a reading sequence is the following:

0x55 0x33 0x02 0x02

In this case: 0x55 – read/write code on the I2C bus; 0x33 – slave address of the finger (0x32) + Read bit; 0x02 – register/function to read from; 0x02 – number of bytes expected to be returned by the finger.

Based on the provided communication capabilities, communication with registers is implemented, such that each register is a separate function in the operation of the finger. Some of the functions include initialization, home and end position of the finger, folding/unfolding of a finger by the operator, setting a position which the finger should autonomously reach, reading the current position, and others. In the table above (Table II) the different commands can be seen with an example of how to use them.

TABLE II
I2C REGISTERS FOR FINGER CONTROL

I2C register	*R/W bit*	*Read/Write Bytes*	*Description*	*USB ISS example*
Manual set - finger movements				
0x01	W	1	Data 0x01 - bending	0x55 0xXX 0x01 0x01 0x01
			Data 0x02 - relieve	0x55 0xXX 0x01 0x01 0x02
0x02	R	2	Read current position of the finger in LSB	0x55 0x(XX+R bit) 0x02 0x02
Manual set - Set limits				
0x03	W	1	Data 0x01 - set home position	0x55 0xXX 0x03 0x01 0x01
			Data 0x02 - set end position	0x55 0xXX 0x03 0x01 0x02
Auto bending				
0x04	W	1	Data 0x01 - go to home position	0x55 0xXX 0x04 0x01 0x01
			Data 0x02 - go to end position	0x55 0xXX 0x04 0x01 0x02
Change I2C id				
0x05	W	1	Change slave address ID	0x55 0xXX 0x05 0x01 0x32
0x06	R	2	Read programmed home position in LSB	0x55 0x(XX+R bit) 0x06 0x02
0x07	R	2	Read programmed end position in LSB	0x55 0x(XX+R bit) 0x07 0x02
Set to position: ***600*** **[***software values corresponding to the resistance of the encoder* ***– least significant bit]***				
0x08	W	2	Move to position in LSB	0x55 0xXX 0x08 0x02 **0x58 0x02**

IV. DEVELOPED SOFTWARE

For the purpose of testing the functionality of the fingers and the hand, a specialized software interface, Fig. 7, was developed using the LabVIEW environment. One of the advantages of “National Instruments – Labview” is in its integration in laboratory and hardware-oriented applications. It is one of the platforms, in terms of easiness and flexibility, which is suitable of proving the software and hardware concepts of the hand. Also, in many of our development projects are included students, who find the graphical programing more intuitive, especially if they don’t have any previous software experience. Currently the program can control only one finger at a time, but it is enough for testing purposes. First the hand is connected to a computer using a USB cable and to the external power supply. Then the corresponding COM serial port is selected, created by the USB-ISS master device, and the “Init” button is clicked to establish a connection. The ID of the finger to be moved is set in the “Finger I2C address” field.

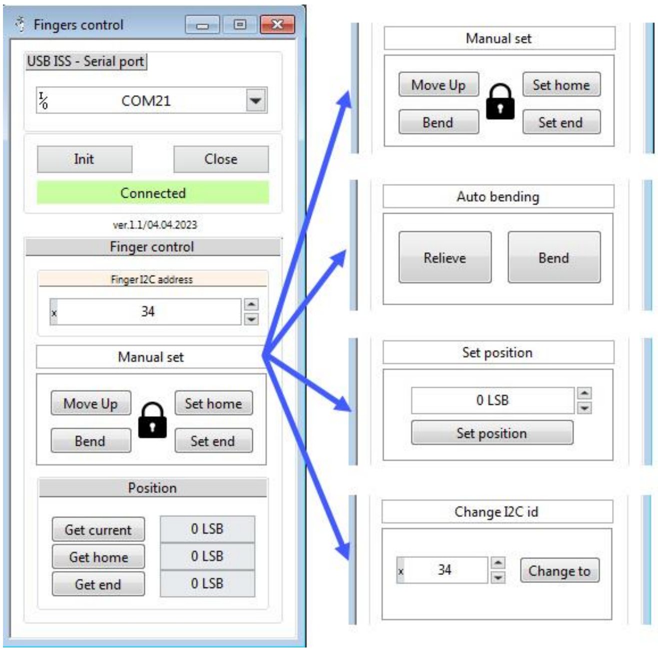

Fig. 7. Software interface for control of the fingers.

Each new finger goes through a one-time initialization process. Each new finger module is preprogrammed with a base ID of 0x32 and it has to go through a one-time initialization process. The new address is reprogrammed using the *“Change I2C ID”* menu, depending on finger position. When assembling each finger, the orientation of the encoder can vary, thus the *home* and *end* limit positions of the new modules have to be set. For this procedure, the operator manually moves the finger to its fully unfolded position which is set as *home* and then to fully folded configuration, which is set as *end*. The controller identifies the position based on the encoder resistance. All parameters from the initialization process are stored in the EEPROM memory.

The program has four different menus with specific functionalities:

Manual set – in this menu the operator can manually fold and unfold a finger using the “Move up” and “Bend” buttons. Under normal conditions, the finger moves if it is between the home and end positions. If it goes outside the range the movement is stopped. When performing the initialization it might be necessary to move the finger outside the limits. In this case the user needs to click the unlock button to enable it. In this menu there are also buttons for setting home/end positions of the finger;

Auto bending – this menu has two options. When selecting either of the two, the finger automatically moves to home or the end position and stops when it reaches it. This function is also used during power-up position initialization.

Set position – A specific number is entered in the field that is between the home and end limits. After clicking “Set position”, Fig.7, the finger automatically moves to the specified position and stops.

Change I2C ID – allows the changing the I2C address (slave id) of the corresponding finger.

Current (Get current) and boundary positions (Get home/Get end) can be read from the software and visualized to the operator for reference.

These numbers are to the least significant bit (LSB) value in the software and corresponds to the current resistance of the encoder.

The motion control is closed-looped by the resistive encoder mounted to the motor shaft. The finger position is completely determined by this type of feedback. The finger free motion is possible within programed boundary positions “*home*” and “*end*” and automatically stops even if the operator requests movements exceeding these critical points. The current prototype does not have force sensors, which are important components in terms of improvement of safety and object handling. The focus of the current version of the fingers/hand is on the mechanical concept and basic motion control. Future improvements are considered by covering the top phalanges with tactile sensors and measuring the motors’ current as proportional to the grasping force.

Since the hand is designed on a modular basis, it is very important that the developed software allows precise examination of an individual module/finger. The current version of the software allows the necessary independent control of the fingers one by one. The software development continues to allow simultaneous finger control.

V. Experiments And Results

The created 3D CAD model of the hand is used to 3D-print the directly assembled modular fingers, base, and cover. Fig. 8 a) and b) represent one finger with its components and the assembled hand without cover of the palm for better clarity.

Human fingers have 3 rotational joints each (the thumb is different and is often modeled with more joints). However, it is difficult for a person to control these joints independently and separately. Fig. 9 positions 2 and 3 are examples of finger phalanga configurations that most people cannot achieve and are also not suitable for grasping objects.

Therefore, it is better to aim for movements of the modular fingers similar to position 1 and to avoid configurations 2 and 3. This effect is achieved by adjusting the initial compression of spring 12 and the initial lengths of the elastic elements 13 (Fig. 1). The distances L_1 and L_2 from Fig. 3 determine the initial tension of elastic elements 13. These distances are obtained experimentally by initially printing several fingers and conducting experiments to achieve the desired folding sequence of the phalanges. The movement pattern of the phalanges is observed and several consecutive measurements are taken. For this purpose, markers are placed on a finger (points P0, P1 to P5) Fig. 10.

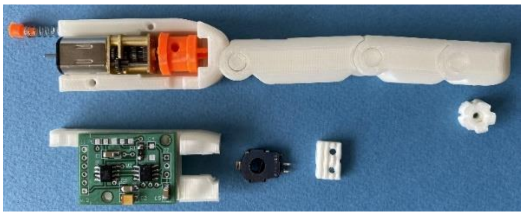

a)

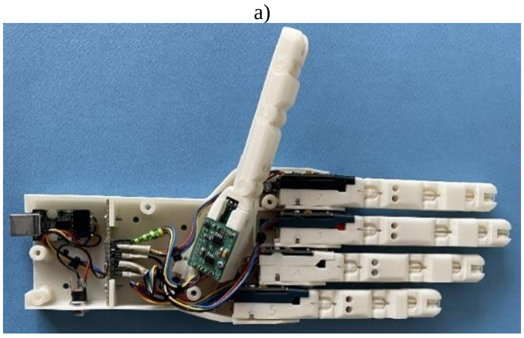

b)

Fig. 8. a) 3D printed finger with main components; b) 3D printed assembled hand without palm cover.

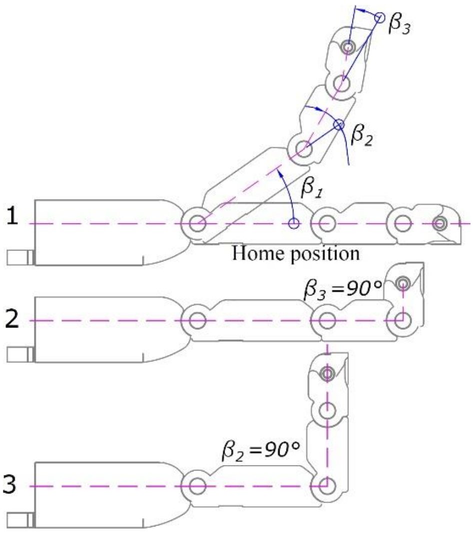

Fig. 9. 1- Home position and configuration where the joints are rotated at different angles; 2 and 3 - configurations that are difficult for humans to achieve.

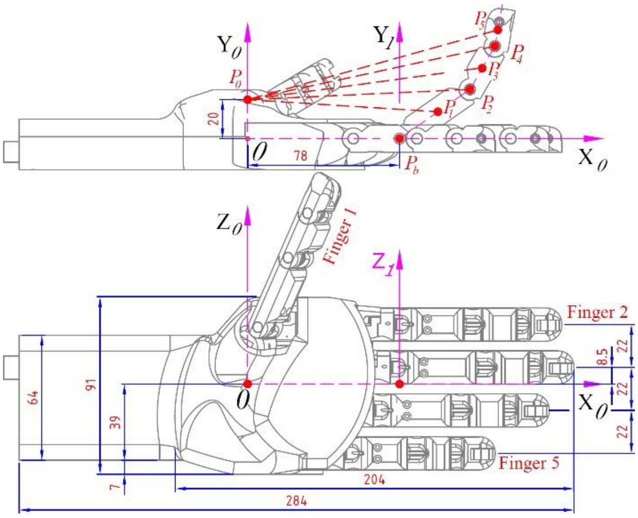

a)

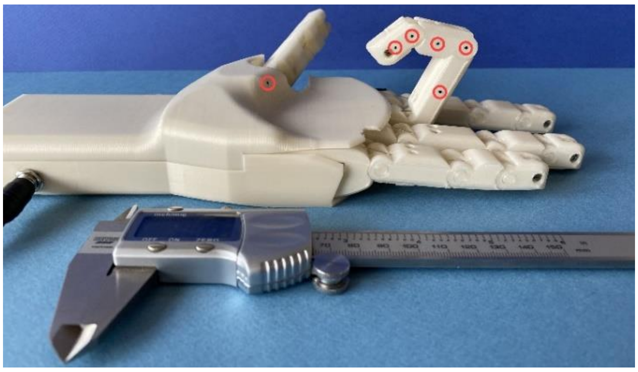

b)

Fig. 10. Location of the points on a finger.

The distances from P_0 to P_1; P_0 to P_2; P_0 to P_3; P_0 to P_3; P_0 to P_5 are measured and are plotted in Table III. These measurements are made for 4 different positions of the finger, with 5 repetitions for each position. The different positions correspond to different angles of rotation of the drum 3 (Fig. 1) and are set in the “Set position” dialog window in the software (Fig. 7). The experiment was carried out with the following four values: 610, 550, 470, 300. The largest value 610 corresponds to the least folding of the finger, and the smallest 300 for the most folded position - Fig. 11. These two values are not the end positions of the finger. The values correspond to a certain resistance of the resistive encoder and are reached automatically by the software. With each repetition, the finger is returned to the home position, after which the folding to the set value takes place. Complete bending and unfolding of one finger can be seen on the video 3.

The rotation of the drum causes folding or unfolding of the finger, as the movements of the individual phalanges are carried out sequentially depending on many factors, such as coefficients of elasticity of the spring and elastic elements, arrangement of the thread, etc. The angles of the individual finger phalanges cannot be controlled independently. The experiment performed shows the current sequence of movements and gives us important guidelines for small changes in the design in order to achieve a desired result close to the dependent movements of the fingers of the human hand.

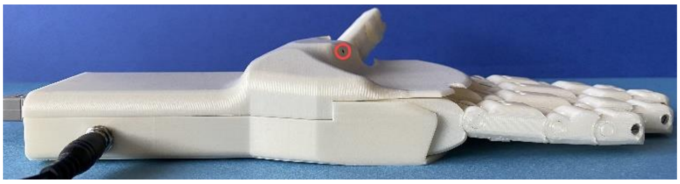

a)

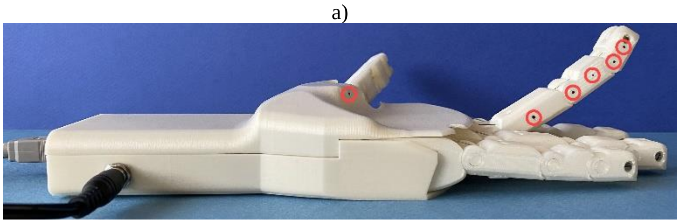

b)

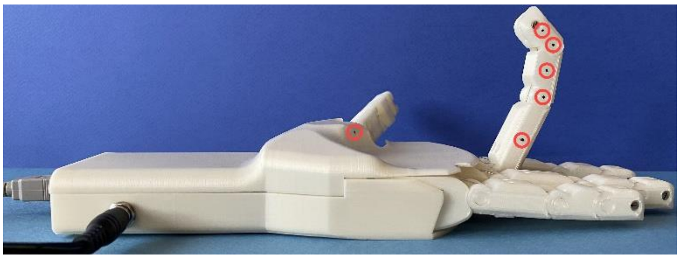

c)

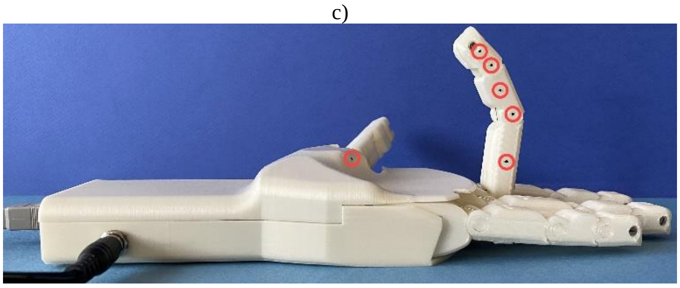

d)

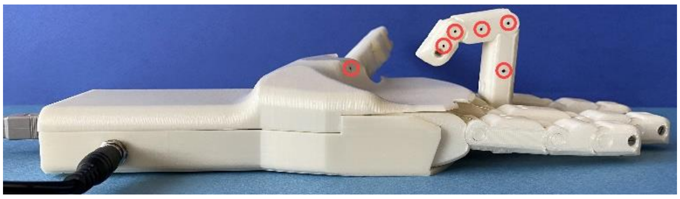

e)

Fig. 11. Positions of the finger, corresponding to the values set in the software. a) – home position; b) – 610; c) – 550; d) – 470; e) – 300.

TABLE III
DISTANCE FROM P0 TO P1, P2, P3, P4 AND P5 FOR DIFFERENT FINGER POSITIONS AND 5 REPETITIONS FOR EACH POSITION

Attempt	*Distance from point P0 to points:*				
	P1 [mm]	*P2 (axis) [mm]*	*P3 [mm]*	*P4 (axis) [mm]*	*P5 [mm]*
	Set position - 610				
1	90,70	109,20	116,07	124,62	130,24
2	91,21	110,13	117,14	125,90	130,43
3	90,77	109,25	116,24	124,79	130,52
4	90.81	109,36	116,27	124,82	129,51
5	91,16	109,94	116,94	125,68	129,82
6	90,71	109,94	116,98	125,78	130,30
7	91,05	109,98	116,50	125,49	130,42
8	90,81	109,86	116,45	125,52	129,67
9	90,86	109,33	116,63	125,28	129,75
10	90,89	109,56	116,99	125,92	130,06
11	90,82	109,41	117,04	125,15	129,76
12	90,73	109,76	117,01	125,61	129,90
13	90,78	109,61	116,48	125,16	129,53
14	91,09	109,97	116,12	124,70	129,80
15	90,83	109,93	116,46	124,77	129,81
16	91,25	110,06	116,21	124,59	129,64
17	90,97	110,21	116,23	125,01	129,62
18	91,20	109,82	116,26	125,46	129,46
19	91,01	110,00	117,00	124,66	130,54
20	90,70	109,64	116,77	125,82	130,45
Max deviation	0,51	0,93	1,07	**1,28**	1,01
Median	90,85	109,84	116,49	125,22	129,82
Std. Dev.	0,19	0,31	0,36	**0,47**	0,37
	Set position - 550				
1	83,46	96,61	93,60	94,04	97,37
2	83,27	96,33	94,41	95,61	99,22
3	83,28	96,24	95,11	97,14	99,06
4	83,31	96,35	95,48	97,83	100,08
5	83,35	96,48	95,68	98,12	99,94
6	83,43	96,39	95,46	94,43	98,29
7	83,38	96,55	94,83	94,9	98,05
8	83,42	96,63	95,23	97,32	99,06
9	83,28	96,24	95,11	97,14	99,06
10	83,26	96,44	94,64	95,12	99,3
11	83,44	96,56	94,68	94,89	99,89
12	83,31	96,35	95,48	97,83	100,08
13	83,29	96,64	95,02	94,49	99,43
14	83,35	96,53	93,8	96,77	99,57
15	83,45	96,51	94,49	94,64	97,4
16	83,4	96,57	93,79	95,4	98,01
17	83,37	96,47	95,09	95,11	98,94
18	83,48	96,6	94,36	96,61	97,38
19	83,27	96,62	94,42	94,13	99,11
20	83,36	96,4	94,41	95,37	98,8
Max deviation	0,19	0,37	2,08	**4,08**	2,71
Median	83,37	96,52	94,66	95,25	99,00
Std. Dev.	0,07	0,12	0,63	**1,37**	0,86
	Set position - 470				
1	82,97	95,41	85,19	77,44	69,28
2	81,53	93,27	82,58	73,81	72,57
3	82,40	94,43	83,74	75,01	70,07
4	82,67	94,86	84,00	75,51	73,69
5	82,30	94,27	83,29	74,67	73,54
6	82,03	94,95	84,23	74,74	71,8
7	82,56	93,75	84,86	74,88	72,66
8	81,57	94,97	83,16	74,16	72,81
9	82,29	93,88	82,95	75,99	73,23
10	81,82	95,02	84,35	75,57	72,61
11	81,79	94,23	83,79	75,34	71,71
12	81,95	94,37	84,3	77,38	70,99
13	82,83	95,31	85,12	74,52	70,53
14	82,57	94,72	83,95	76,5	72,02
15	82,09	93,32	83,73	74,93	71,37
16	81,63	93,59	83,32	74,07	70,12
17	82,62	93,72	83,17	75,21	72,48
18	82,43	94,61	85,18	75,31	70,37
19	81,93	94,89	84,03	74,85	72,22
20	82,02	93,95	83,84	76,37	71,2
Max deviation	1,44	2,14	2,61	3,63	**4,41**
Median	82,19	94,40	83,90	75,11	71,91
Std. Dev.	0,43	0,65	0,75	1,00	**1,24**
	Set position - 300				
1	73,45	78,19	65,32	53,19	45,46
2	74,08	79,17	66,21	54,18	46,41
3	74,04	79,34	66,33	54,50	46,57
4	74,09	79,51	66,53	54,64	46,82
5	74,14	79,48	66,54	54,48	46,74
6	73,89	79,43	65,83	53,76	45,8
7	74,12	78,88	66,11	53,52	46,52
8	74,18	78,8	65,64	54,29	46,64
9	73,9	78,91	65,57	53,82	46,62
10	74,13	79,08	65,66	53,78	45,59
11	74,03	79,24	65,78	54,12	46,7
12	74,16	78,92	65,99	54,16	46,59
13	73,85	78,84	66,31	54,07	45,54
14	74,15	78,71	66,02	54,11	46,22
15	73,91	78,64	66,51	54,03	46,16
16	73,95	78,78	65,69	53,48	46,67
17	74,06	79,26	65,65	53,66	45,77
18	74,07	79,32	66,32	53,65	45,87
19	74,09	79,48	65,81	53,8	46,57
20	73,86	79,04	66,13	54,51	45,55
Max deviation	0,69	1,32	1,22	**1,45**	1,36
Median	74,07	79,06	66,01	54,05	46,47
Std. Dev.	0,17	0,34	0,36	0,39	**0,48**

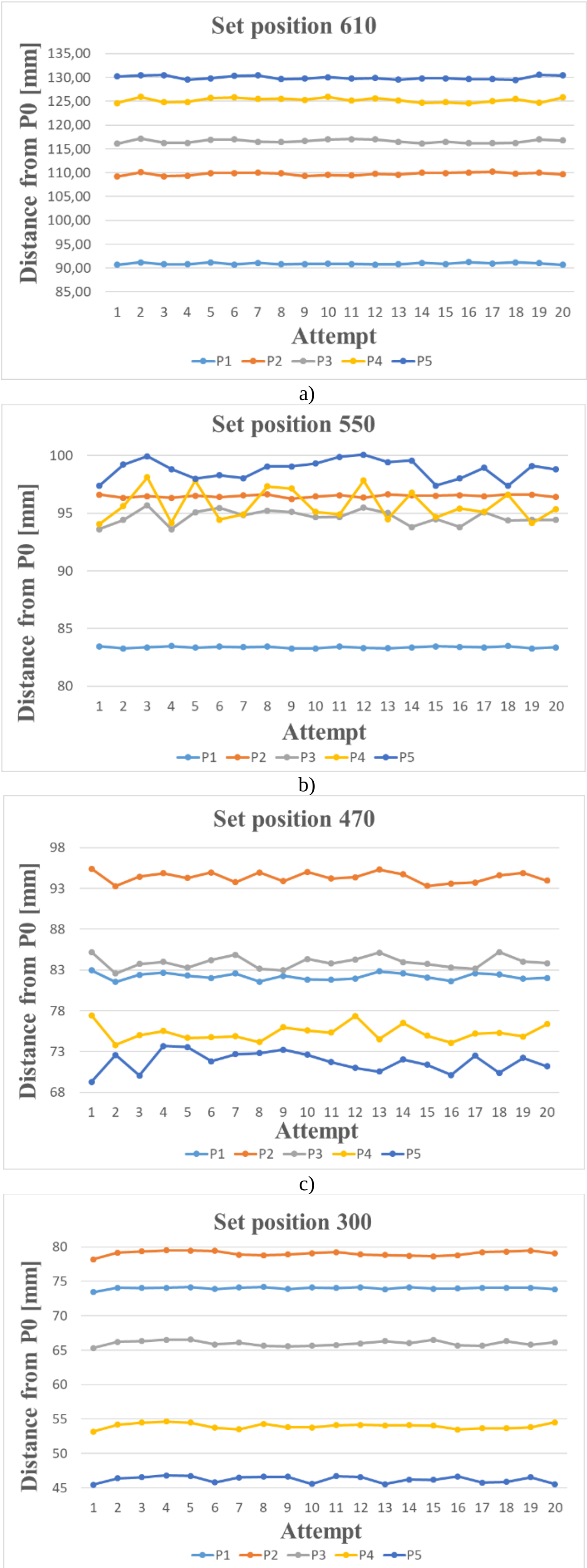

Fig. 12. Plots of the repetitions for the four different finger positions at values of a) 610, b) 550, c) 470 and d) 300.

Fig. 13. Experimental setup for measuring the maximum force that can be applied by the tip of each finger.

The results from measurements are given in Table III.

With the experiment the repeatability of the already assembled and functioning finger can be analyzed; the measured values are visualized in the graphs of Fig. 12. It can be seen from the graphs and Table III that the maximum deviations in [mm] at the positions with values 610 and 300 are 1.28[mm] and 1.45[mm], respectively. Therefore, these are the most stable positions of those studied, and repeatability is guaranteed to a higher degree. The positions corresponding to values 550 and 470 can be considered intermediate and the graphs show that they are not as stable, with the largest deviation being 4.41 [mm] for the position with value 470. The values of the standard deviotion for those positions are also the highest. These findings are important for the different applications of the hand: grasping of various objects, visualization of gestures, and others.

The second experiment conducted with the prototype measures the maximum force realized by the fingertips. The hand is held stationary with a fixture stand and an operator moves each finger to a position where the tip touches and exerts a force on an electronic scale (Fig. 13). The corresponding results are given in Table IV.

TABLE IV
MAXIMUM FORCE APPLIED BY EACH FINGERTIP

Finger	Measured value [gr.]	Force [N]
1 thumb	48	0.48
2 forefinger	36	0.36
3 middle finger	32	0.32
4 ring finger	38	0.38
5 little finger	50	0.50

From the table it can be seen that the greatest force of 0.5[N] is realized by the shortest finger. This is because the same type of motor drives the fingers and exerts the same torque on fingers of different lengths. This is also the reason why the result might not correspond to human fingers, which are driven by different sized muscles. This data is useful for relevant applications of the hand, such as pressing keys on a keyboard, or pressing various buttons and elements.

IV. Concluding Remarks

A new design of a 3D-printed hand with modularly designed fingers is presented. It includes fingers that are built directly assembled using 3D printing technology, which saves one technological operation – the assembly process. It also allows manufacturing to be easily performed anywhere directly from the 3D model without the need for drawing documentation. The modules include not only the mechanical components but also the motor, the controller, and the sensor feedback system.

The presented experimental results show that the fingers work reliably and that it is possible to control the folding sequence of individual phalanges by changing the characteristics of the elastic elements. This can be done smoothly by regulating the spring which is responsible for the most heavily loaded joint and by regulating the distances L_1 and L_2 (Fig. 3). The proposed experiment allows for the tracking of the folding sequence of the phalanges and, if necessary, the correction of the indicated functional elements. On the other hand, the proposed method of measurement and the results given in Fig. 12 and Table enable the determination of the repeatability of movements after multiple repetitions.

The modular design of the mechanical and control components has a number of advantages: it allows for easy replace a complex finger in the event of damage or wear; the reliability of the finger increases; production is facilitated; it is possible to design hands with different numbers of fingers, etc.

Development of the hand's sensory system and improvement of the control will be completed in the sequel. The mechanical design will be improved by designing a thumb with more degrees of freedom and by adding degrees of freedom at the wrist. New materials for the production of the hand will be investigated to improve its strength and wear resistance. The next stage of software development will include simultaneous control of several fingers and planning the movements of the fingers when grasping objects of different shapes and sizes.
This work presents new directions for the development of the 3D-printed model. In addition, the results are believed to be useful for other researchers who are developing 3D-printed humanoid hands. The development of the project is shared in the following platform: https://github.com/prelibiton/3D-printed-humanoid-hand/tree/main.

Acknowledgment

This work was supported by the European Regional Development Fund within the OP “Science and Education for Smart Growth 2014–2020”, Project CoC “Smart Mechatronic, Eco-And Energy Saving Systems And Technologies”, № BG05M2OP001-1.002-0023.

References

[1] Eric Deng, Yonas Tadesse, A Soft 3D-Printed Robotic Hand Actuated by Coiled SMA. Actuators 2021, 10, 6. https://doi.org/10.3390/act10010006.

[2] Jan Koprnický, Petr Najman and Jiří Šafka, "3D-printed bionic prosthetic hands," 2017 IEEE International Workshop of Electronics, Control, Measurement, Signals and their Application to Mechatronics (ECMSM), Donostia, Spain, 2017, pp. 1-6, doi: 10.1109/ECMSM.2017.7945898.

[3] Ivan Chavdarov, Ivajlo Georgiev, Bozidar Naydenov and Valentin Nikolov, "Design of a 3D-printed Humanoid Robotic Hand", 2023 International Conference on Software, Telecommunications and Computer Networks (SoftCOM), Split, Croatia, 2023, pp. 1-6, doi: 10.23919/SoftCOM58365.2023.10271644.

[4] Dorijan Sablic-Nemec and Miroslav Joler, "An Automated Approach to Horn Antenna Impedance Matching and Manufacturing Using 3D Printing," in Journal of Communications Software and Systems, vol. 19, no. 3, pp. 188-198, July 2023, doi: 10.24138/jcomss-2023-0100.

[5] Pascal Weiner, Julia Starke, Samuel Rader, Felix Hundhausen, Tamim Asfour, Designing Prosthetic Hands With Embodied Intelligence: The KIT Prosthetic Hands. Front Neurorobot. Volume 16-2022, 10;16:815716. doi: 10.3389/fnbot.2022.815716.

[6] Yancharo Wang, Ye Tian, Haotain She, Y. Jiang, H. Yokoi, Y. Liu. Design of an Effective Prosthetic Hand System for Adaptive Grasping with the Control of Myoelectric Pattern Recognition Approach. Micromachines (Basel). 2022 Jan 29;13(2):219. doi: 10.3390/mi13020219.

[7] T. Mouri, H. Kawasaki, T. Aoki, Y. Nishimoto, S. Ito, and S. Ueki, “Telerehabilitation for fingers and wrist using a hand rehabilitation support system and robot hand,” in Proceedings of the 9th International Symposium on Robot Control, pp. 751–756, September 2009.

[8] M. Hioki, H. Kawasaki, H. Sakaeda, Y. Nishimoto, and T. Mouri, “Finger rehabilitation support system using a multifingered haptic interface controlled by a surface electromyogram,” J. of Robotics, Article ID 167516, 2011.

[9] L. Bridgwater, C. Ihrke, M. Diftler, M. Abdallah, N. Radford, J. Rogers, S. Yayathi, R. Askew, and D. Linn, “The robonaut 2 hand-designed to do work with tools,” in 2012 IEEE International Conference on Robotics and Automation, pp. 3425–3430, IEEE, 2012.

[10] H. Park, D. Kim, “An open-source anthropomorphic robot hand system: HRI hand”, HardwareX, Volume 7, 2020, e00100, ISSN 2468-0672, https://doi.org/10.1016/j.ohx.2020.e00100.

[11] I. Chavdarov, P. Dachikov, G. Elenchev, R. Iliev, I. Stoyanov, S. Mincheva, A. Krastev, “3D-printed humanoid hand”, Proceedings of the International Conference “Robotics & Mechatronics and Social Implementations”, pp. 107-11, 2018.

[12] Z. Xu, V. Kumar and E. Todorov, "A Low-cost and Modular, 20-DOF, Anthropomorphic Robotic Hand: Design, Actuation and Modeling.", 13th IEEE-RAS International Conference on Humanoid Robots (Humanoids), Atlanta, GA, October 15 -17, 2013.

[13] V. Kumar, Z. Xu, and E. Todorov, “Fast, strong and compliant pneumatic actuation for dexterous tendon-driven hands,” in 2013 IEEE International Conference on Robotics and Automation, 2013.

[14] J. Chapman, A. Dwivedi and M. Liarokapis, "A Dexterous, Adaptive, Affordable, Humanlike Robot Hand: Towards Prostheses with Dexterous Manipulation Capabilities," 2022 IEEE-RAS 21st International Conference on Humanoid Robots (Humanoids), Ginowan, Japan, 2022, pp. 337-343, doi: 10.1109/Humanoids53995.2022.10000237

[15] N. E. Nava Rodrı´guez , G. Carbone, M. Ceccarelli, Optimal design of driving mechanism in a 1-DOF anthropomorphic finger, Mechanism and Machine Theory 41 (2006) 897–911

[16] Wu, C.; Song, T.; Wu, Z.; Cao, Q.; Fei, F.; Yang, D.; Xu, B.; Song, A. Development and Evaluation of an Adaptive Multi-DOF Finger with Mechanical-Sensor Integrated for Prosthetic Hand. Micromachines 2021, 12, 33. https://doi.org/10.3390/mi12010033

[17] R. Johansson, A. Vallbo. Tactile sensibility in the human hand: relative and absolute densities of four types of mechanoreceptive units in glabrous skin. J Physiol. 1979 Jan;286:283-300. doi: 10.1113/jphysiol. 1979.sp012619. PMID: 439026; PMCID: PMC1281571.

[18] L. Dunai, M. Novak, C. García Espert, Human Hand Anatomy-Based Prosthetic Hand. Sensors (Basel). 2020 Dec 28;21(1):137. doi: 10.3390/s21010137.

[19] V. Stornelli, A. Leoni, G. Ferri, V. Errico, A. Pallotti, G. Orengo and G. Saggio, "A 10-17 DOF Sensory Gloves with Harvesting Capability for Smart Healthcare," in Journal of Communications Software and Systems, vol. 15, no. 2, pp. 166-172, April 2019, doi: 10.24138/jcomss.v15i2.693.

[20] J. Zhou, X. Chen, U. Chang, J. Pan, W. Wang and Z. Wang, "Intuitive Control of Humanoid Soft-Robotic Hand BCL-13," 2018 IEEE-RAS 18th International Conference on Humanoid Robots (Humanoids), Beijing, China, 2018, pp. 314-319, doi: 10.1109/HUMANOIDS.2018.8624947.

[21] S. Pohtongkam, J. Srinonchat. Tactile Object Recognition for Humanoid Robots Using New Designed Piezoresistive Tactile Sensor and DCNN. Sensors. 2021; 21(18):6024. https://doi.org/10.3390/s21186024.
[22] P. Scarfe, E. Lindsay, Air Muscle Actuated Low Cost Humanoid Hand. International Journal of Advanced Robotic Systems. 2006;3(2). doi:10.5772/5745.
[23] P. Weiner, C. Need, Y.Shibata, Y. Nakamura, T. Asfour, "An embedded, multi-modal sensor system for scalable robotic and prosthetic hand fingers," Sensors, vol. 20, no. 1, 2020.
[24] V. Nikolov, I. Georgiev and I. Chavdarov, "Hardware and software of a 3D-printed humanoid hand," 2023 XXXII International Scientific Conference Electronics (ET), Sozopol, Bulgaria, 2023, pp. 1-6, doi: 10.1109/ET59121.2023.10278809.
[25] M. Krawczyk, V. Gandhi, Z. Yang. (2022). Robot Operating System (ROS) Controlled Anthropomorphic Robot Hand. Journal of Scientific and Industrial Research. 81. 901-910.10.56042/jsir.v81i09.45313.
[26] M. Tetsuya, K. Haruhisa,Yoshikawa, K., Takai, J.,Ito, Soken. (2002). Anthro,pomorphic robot hand: Gifu hand III. Proc. of Int. Conf. ICCAS2002. 1288-1293.
[27] D. Hanson, I. Alishba, G. Morales, V. Krisciunas, A. Sagi, A. Malali, R. Mohbe, R. Upadrashta, (2022). Open Arms: Open-Source Arms, Hands & Control. 10.48550/arXiv.2205.12992.
[28] H. Wang, F. J. Abu-Dakka, T. Nguyen Le, V. Kyrki and H. Xu, "A Novel Soft Robotic Hand Design With Human-Inspired Soft Palm: Achieving a Great Diversity of Grasps," in IEEE Robotics & Automation Magazine, vol. 28, no. 2, pp. 37-49, June 2021, doi: 10.1109/MRA.2021.3065870.
[29] Z. Ren, N. Kashiri, C. Zhou and N. G. Tsagarakis, "HERI II: A Robust and Flexible Robotic Hand based on Modular Finger design and Under Actuation Principles," 2018 IEEE/RSJ International Conference on Intelligent Robots and Systems (IROS), Madrid, Spain, 2018, pp. 1449-1455, doi: 10.1109/IROS.2018.8594507.
[30] L. Liow, A. B. Clark and N. Rojas, "OLYMPIC: A Modular, Tendon-Driven Prosthetic Hand With Novel Finger and Wrist Coupling Mechanisms," in IEEE Robotics and Automation Letters, vol. 5, no. 2, pp. 299-306, April 2020, doi: 10.1109/LRA.2019.2956636.
[31] I. Chavdarov, "A robotic humanoid arm", Patent N 67070 B1/12.06.2020, http://www1.bpo.bg/images/stories/buletini/binder-2017-09.pdf
[32] V. Sureshbabu, G. Metta and A. Parmiggiani, "A Systematic Approach to Evaluating and Benchmarking Robotic Hands—The FFP Index". Robotics 2019, 8, 7. https://doi.org/10.3390/robotics8010007
[33] S. Sampath, N. Wang, H. Wu and C. Yang, "Review on human-like robot manipulation using dexterous hands", Cognitive Computation and Systems, vol. 5, Issue1, March 2023, Pages 14-29, https://doi.org/ 10.1049/ccs2.12073
[34] T. Mouri, H. Kawasaki, K. Yoshikawa, J. Takai and S. Ito. "Anthropomorphic robot hand: Gifu hand III". 2002, Proc. of Int. Conf. ICCAS2002. 1288-1293
[35] T. Chen, X. Zhao, G. Ma, et al. "Cable Driven Humanoid Hand". Chin. J. Mech. Eng. 34, 76 (2021). https://doi.org/10.1186/s10033-021-00595-y

Ivan Chavdarov got a B.S. degree in mechanical engineering in 1991 from the Technical Sofia University. He received his Ph.D. in "Robots and manipulators" and became an associate professor in the Institute of Robotics, Bulgarian Academy of Sciences. In 2017 he became an associate professor in the "Mechatronics, Robotics and Mechanics" department of the Sofia University, "St. Kliment Ohridski". His interests include the mechanics and design of mobile and stationary robots. He has 10 patents in the field of mechatronics. He is interested in using a minimalistic approach in robot design and the application of innovative constructions based on 3d printing technology.

Bozhidar Naydenov received his M.S. degree in Industrial Engineering from the Technical Sofia University in 2011. He received his Ph.D. in "Robots and manipulators" from the Institute of Robotics, Bulgarian Academy of Sciences in 2015.
His research interests include the mechanics and design of mobile robots and robotized devices for extracting energy from sea waves. His interests also focus on 3D printing technologies and their application for innovative robot design.

Valentin Nikolov received a M.S degree of Automation in 2011 and Ph.D. in "Robots and manipulators" in 2010, both from Technical Sofia University. Since 2007 works in Sensata Technologies as R&D, equipment build and software engineer as the focus of work is automotive engineering, data processing, automation, e-mobility. Since 2010 is a part of robot research engineering team in Institute of Robotics, Bulgarian Academy of Science. The focus of his interests are mobile and biologically inspired robots, AI and its application of robots control, human-machine interfaces, prosthesis.

Ivaylo Georgiev graduated in 2016 with a bachelor in Computer Science and in 2019 with master in Embedded Systems from the Sofia university. He is currently PhD candidate at the Bulgarian Academy of Sciences - Institute of Robotics. Since 2017 he is working as a software developer in MM Solutions. His interests include robotics, bio engineering, prosthetic devices and 3d printing.